

See discussions, stats, and author profiles for this publication at: <https://www.researchgate.net/publication/361298398>

A Study of Interference Analysis Between mmWave Radars and IEEE 802.11AD at 60 GHz Bands

Article in *International Journal of Wireless Information Networks* · September 2022

DOI: 10.1007/s10776-022-00564-9

CITATIONS

3

READS

520

6 authors, including:



Kaveh Pahlavan

Worcester Polytechnic Institute

394 PUBLICATIONS 11,289 CITATIONS

[SEE PROFILE](#)



Haowen 'John' Wei

Columbia University

5 PUBLICATIONS 28 CITATIONS

[SEE PROFILE](#)



Seyed Zekavat

Michigan Technological University

215 PUBLICATIONS 2,771 CITATIONS

[SEE PROFILE](#)



A Study of Interference Analysis Between mmWave Radars and IEEE 802.11AD at 60 GHz Bands

Shiyu Cheng¹ · Kaveh Pahlavan¹ · Haowen Wei¹ · Zhuoran Su¹ · Seyed Reza Zekavat² · Ali Abedi³

Received: 1 September 2021 / Revised: 9 May 2022 / Accepted: 16 May 2022
© The Author(s), under exclusive licence to Springer Science+Business Media, LLC, part of Springer Nature 2022

Abstract

This paper presents an empirical analysis of the mutual interference between the IEEE 802.11ad communication link and the Texas Instruments (TI) millimeter wave (mmWave) radar in 60 GHz bands. We study the impact of IEEE 802.11ad communication link on the mmWave radar coverage and precision, and we model the impact of mmWave radar interference on the IEEE 802.11ad wireless communication packet loss rate. The paper investigates interference based on the angle between the interfering multiple input multiple output (MIMO) beamforming antennas of the two devices. We benefit from the Cramer-Rao Lower Bound for the analysis of precision degradations of the mmWave radar due to interference from the IEEE 802.11ad, and we benefit from empirical path-loss models to analyze the impact of the interference on coverage of the radar. We measure the empirical packet loss rate of the IEEE 802.11ad due to the interference from the mmWave radar in a laboratory testbed.

Keywords IEEE 802.11ad · mmWave radar · Interference analysis · Modeling

1 Introduction

Recently, intelligent spectrum management and regulations for exponentially growing number of radio frequency (RF) devices have attracted considerable attention to enable a new paradigm in spectrum management [1]. The evolution

of the new paradigms in intelligent spectrum management demands more in-depth understanding of interference analysis among these RF devices. Two major categories of RF devices are wireless communications devices like Wi-Fi and cellular networks, and wireless positioning devices like radars. Cellular networks and long range radars operate in *licensed bands*, while Wi-Fi and short-range radars operate in *unlicensed bands*. Interference is inherent to unlicensed band operation when devices are in the proximity of each other. Analysis of this interference is complex because it involves physical and medium access control of the RF communication devices as well as details of signal design for radars. The mmWave devices have emerged to address spectrum scarcity. Both IEEE 802.11ad and mmWave radar operate in the unlicensed mmWave 60 GHz band.

IEEE 802.11ad standard operates in mmWave unlicensed band to support multi Gbps throughput [2]. This standard uses beamforming with MIMO antennas to deal with the problem of high attenuation and the exponentially growing demand on the data rate. Benefitting from the multi Gbps throughput of the IEEE 802.11ad, many novel applications have been developed. With the emergence of IEEE 802.11ad devices, large documents can be downloaded from the cloud with minimal delay, video games benefitting from virtual

✉ Shiyu Cheng
scheng3@wpi.edu

Kaveh Pahlavan
kaveh@wpi.edu

Haowen Wei
hwei@wpi.edu

Zhuoran Su
zsu2@wpi.edu

Seyed Reza Zekavat
rezaz@wpi.edu

Ali Abedi
ali.abedi@maine.edu

¹ Electrical and Computer Engineering, Worcester Polytechnic Institute, Worcester, USA

² Data Science, Worcester Polytechnic Institute, Worcester, USA

³ Electrical and Computer Engineering, University of Maine, Orono, USA

reality may operate with higher performance, and large files can be exchanged at higher data rates.

In addition, the growth of the wireless networking industry has paved the way to the commercial success of low-cost mmWave radars operating on unlicensed bands. They have been leveraged on modern cyberspace applications such as human–computer interaction, gesture and motion detection, authentication, and security [3]. The mmWave radar operating at 60–64 GHz is a crucial technology on the Internet of things (IoT) for its capability of detecting the range, velocity, and the angles-of-arrival of signals with sub-centimeter range accuracy, and they have been used in the automotive industry for short-range collision detection. The interference generated by these radars could impact mmWave wireless communications devices such as Wi-Fi.

Historically, interference in the unlicensed band was first addressed by the IEEE 802.15.2 to analyze the mutual impacts of IEEE 802.11b and Bluetooth on quality of wireless communications for each of the devices [4]. Some recent works analyze the interference between radar and communication systems working on S-band. Authors in [5] use an experimental study to analyze the interference on commercial cellular communication system from air traffic control radar. A theoretical analysis of interference created by commercial cellular on military radar systems is investigated in [6]. Another set of works focus on the analysis of the interference between communication and frequency-modulated continuous-wave (FMCW) radar, which operate on unlicensed bands. In [7], authors study FMCW radar interference effects on IEEE 802.11n Wi-Fi communication. They set the FMCW radar as the interference source and change the interference to signal power ratio. The research reported in [5]–[7] focus on the wireless systems working on 3.5 GHz and 2.5 GHz bands. In [8], authors address the analysis of the interference between radar and communication systems working on mmWave bands theoretically, without resorting to empirical data for validation of the results. In [9], authors analyze the interference between multiple IEEE 802.11ad operating at 60 GHz on the inter-vehicular communication link quality for applications such as the real-time transmission of high-definition video streams. Authors in [10] assess interference between multiple mmWave radar devices. However, the interference between IEEE 802.11ad and mmWave radars operating at 60 GHz mmWave bands has not received adequate attention.

This paper investigates a methodology for the analysis of the interference between IEEE 802.11ad and TI mmWave Radar operation around 60 GHz where the frequency channels of the two mmWave systems are overlapped. It offers a comprehensive analysis and validates them with an empirical analysis of mutual interference between IEEE 802.11ad wireless communication devices and the mmWave radars operating on 60 GHz unlicensed bands. The paper

examines IEEE 802.11ad and TI mmWave radar interference via designing a testbed. The model of interference is built based on the distance and the angle-of-arrival (AOA) of IEEE 802.11ad communication link. The paper analyzes the influence on the coverage and precision of the radar-based on the signal to the interference ratio (SIR) and Cramer-Rao Lower Bound (CRLB). We demonstrate that when the IEEE 802.11 interference is close to the mmWave radar, the detection range of the radar will decrease significantly, while precision of the radar remains almost the same. An interference time ratio model is used to analyze the increase of the packet loss rate of the IEEE 802.11ad communication when interference from the mmWave radar is introduced. By tuning the frame rate of the radar, we change the time ratio of the interference. The empirical measurement of packet loss rate is compared with the analytical results based on the interference time ratio model. With the increase of the frame rate, the packet loss rate (PLR) increases as well, when the frame rate is 30 frames per second, the experimental PLR is 18% and the analytical PLR is 15.55%.

The rest of this paper is organized as follows. Section II introduces the background of this research by explaining the detailed method of operation of the IEEE 802.11ad and the TI mmWave radar. Section III studies the impact of the IEEE 802.11ad communication link on the coverage and precision of the TI mmWave radar. Section IV investigates the impact of the TI mmWave radar on the packet-loss rate of the IEEE 802.11ad communication link. Section V introduces the future work. Section VI concludes the paper by summarizing the results of the analysis.

2 Background in IEEE 802.11ad and mmWave Radar Interference

The objective of this study is to measure the interference between the IEEE 802.11ad and mmWave radars operating in overlapping frequencies at unlicensed mmWave around 60 GHz bands. The IEEE 802.11ad standard supports wireless communications at unlicensed mmWave band which covers from 57.24 to 70.20 GHz. The frequency band has 6 subdivided channels, and the bandwidth for each channel is $B_c = 2.16$ GHz, which supports the data rate up to 6.75 Gbps. The standard recommends MIMO antenna systems with beamforming capabilities to deal with high attenuations at 60 GHz. To conduct our experiments, we use a pair of IEEE 802.11ad RBwAPG-60ad devices at center frequency of 62.64 GHz, which are manufactured by Mikrotik. The short-range TI mmWave radar operating at 60–64 GHz [11], whose bandwidth is $B_r = 4$ GHz, has also emerged for short range micro-gesture and motion detection [3] as well as short distance ranging [12]. The mmWave radar uses short-wavelength electromagnetic waves to detect objects based

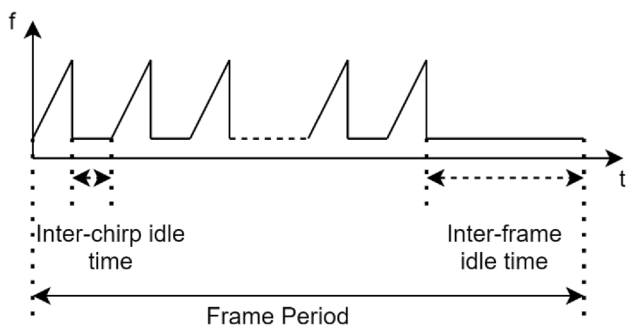


Fig. 1 Frequency-modulated continuous wave (FMCW) chirp radar frame structure for periodic sweep with inter-frame idle times as well as inter-chirp idle times

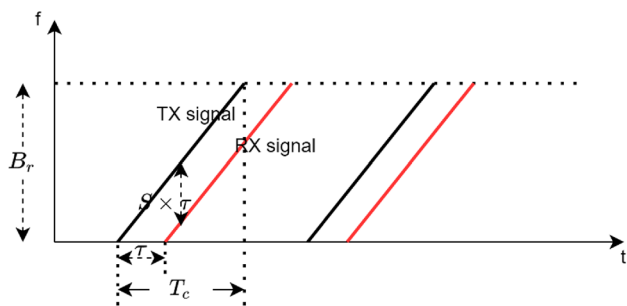


Fig. 2 The time–frequency relation between the transmitted and the received signal and their associated parameters, S is the slope of the chirp and τ is the propagation delay. The difference in transmitted and the received frequencies is $S \times \tau$, used to calculate the distance between objects and the radar

on the transmitted signals and the received signals, which are reflected from objects. These two devices could interfere with each other, when their bands overlap.

To design our testbed, we used the TI’s FMCW mmWave radar, which detects the position of the objects based on the frequencies of the transmitted signal and the received signal. Figure 1 shows the structure of FMCW frames. In linear FMCW radars, the frequency of transmitter (TX) signal changes linearly with time. The signal sweeps the bandwidth which is referred to as a chirp. Between each two chirps, there is an inter-chirp idle time. In each frame, it contains a series of chirps and followed by inter-frame idle time. Frame rate represents the number of frames in one second. As shown in Fig. 2, an FMCW radar transmits a series of chirps and receives signals reflected from an object at the receiver (RX). The RX signal is time delayed but has the same linear ramp form as the TX signal. The FMCW radar mixes the TX signal and RX signal to generate the intermediate frequency (IF) signal, whose frequency is the difference between the instantaneous frequencies of the TX signal and RX signal.

As introduced in [13], the propagation delay is

$$\tau = \frac{2d}{c} \tag{1}$$

where τ is the propagation delay, d is the distance between the radar and the object, and c is the speed of the light.

Therefore, the relationship between the frequency of IF signal and the distance between the radar and the object is

$$f_{IF} = S \times \tau = \frac{2d \times S}{c} \tag{2}$$

where f_{IF} is the frequency of IF signal, S is the slope of the chip, τ is the propagation delay, d is the distance between the radar and the object, c is speed of light.

The range resolution (R_{res}) of FMCW radar is the minimum distance between two different targets for the radar to separate them. According to (2), the difference in their IF frequencies (Δf) is

$$\Delta f = \frac{2\Delta d \times S}{c} \tag{3}$$

where Δd is the distance between two targets. The difference in their IF frequencies should be larger than the reciprocal of the time of the chirp to resolve two signals reflected from two targets:

$$\Delta f > \frac{1}{T_c} \tag{4}$$

where T_c is the duration of a chirp. Therefore,

$$\frac{2\Delta d \times S}{c} > \frac{1}{T_c} \Rightarrow \Delta d > \frac{c}{2 \times S \times T_c} \tag{5}$$

Since the sweep bandwidth of the chirp of the FMCW radar (B_r) corresponds to

$$B_r = S \times T_c \tag{6}$$

where B_r is the sweep bandwidth of the chirp of the FMCW radar.

The range resolution (R_{res}) of FMCW radar is

$$R_{res} = \frac{c}{2B_r} \tag{7}$$

The mmWave radar used in this paper is IWR6843AOPEVM, which works on the 60–64 GHz band. It can be used by vehicles to enjoy a safer driving experience and be used by specific applications to detect human gestures. With the development of the IoT industry, IEEE 802.11ad devices and mmWave radar will be widely used in our daily lives.

3 IEEE 802.11ad Interference to mmWave Radar

In radars, we have two issues which are range and precision. The range is calculated from the signal to the interference plus noise ratio (SINR) and precision is affected by bandwidth, SINR, and measurement time. To analyze the SINR, the power of the radar signal (P_S) and the power of the interference signal (P_I) should be calculated. The signal power is:

$$\begin{cases} P_S = \frac{P_{t_r} G_{TX_r} \sigma G_{RX_r} \lambda_r^2}{(4\pi)^3 d^4} \\ P_S(dB) = -40 \log_{10}(d) + 10 \log_{10} \frac{P_{t_r} G_{TX_r} \sigma G_{RX_r} \lambda_r^2}{(4\pi)^3} \end{cases} \quad (8)$$

where P_{t_r} is the output power of the radar, G_{TX_r} and G_{RX_r} represent the antenna gains of the radar TX and RX, σ is the radar cross-section (RCS) of the object, λ_r is the wavelength of the radar signal, and d is the distance between the object and the radar.

The power of the interference source is

$$\begin{cases} P_I = \frac{P_{t_c} G_{TX_c} G_{RX_c} \lambda_c^2}{4\pi r^2} \\ P_I(dB) = -20 \log_{10} r + 10 \log_{10} \frac{P_{t_c} G_{TX_c} G_{RX_c} \lambda_c^2}{4\pi} \end{cases} \quad (9)$$

where P_{t_c} and G_{TX_c} are the output power and antenna gain of the transmitter of the IEEE 802.11ad device, λ_c is the wavelength of the IEEE 802.11ad communication signal, and r is the distance between the radar and the IEEE 802.11ad transmitter. The value of G_{RX_c} is related to AOA.

Therefore, the SINR is

$$\begin{cases} SINR = \frac{P_S}{P_I + P_N} \approx \frac{P_S}{P_I} \\ SINR(dB) \approx P_S(dB) - P_I(dB) \end{cases}, \quad (10)$$

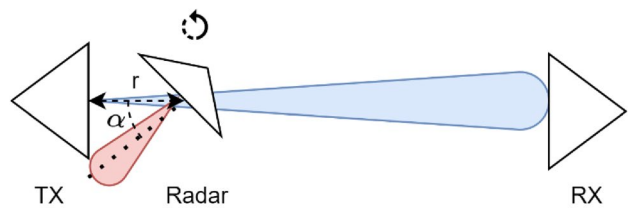
where P_N is the power of thermal noise. In this scenario, since the mmWave radar is close to the IEEE 802.11ad TX, P_I is much stronger than P_N , therefore the thermal noise is negligible.

3.1 A Testbed for Measurement of the SINR

Figure 3 shows the basic scenario for empirical measurement of the received signal at the radar from the IEEE 802.11ad as an object close to the radar when the IEEE 802.11ad is on and off. When the 802.11ad TX is off the received signal at the radar is P_S . In addition, when the IEEE 802.11ad is on, we can measure P_I at the radar. In this scenario, we measure the distance, r , between the IEEE 802.11ad transmitter, which is the interference source as well as the target, and mmWave radar, and AOA, α .



(a)



(b)

Fig. 3 Scenario for the IEEE 802.11ad communication link interference to TI mmWave radar. **a** The IEEE 802.11ad TX is set as the interference source and detected target for the radar. **b** The distance between IEEE 802.11ad TX and RX is fixed as 7.5 m. The distance between the IEEE 802.11ad TX and radar is r . When the TX is turned off, we move the radar away from the TX to measure the P_S ; When the TX is turned on, we move the radar away from the TX and rotate the radar to make the interference signal from IEEE 802.11ad TX has different angle of arrival, and measure the P_I

The testbed is built in a laboratory environment. As shown in Fig. 3, TX and RX are set apart for 7.5 m. To measure P_S , the TX and RX are turned off, the TX is set as the target, the distance between radar and target, r , is changed from 0.6 to 2.1 m. To measure P_I , the TX and RX are turned on, the TX is set as the interference source, the distance between radar and TX, r , is changed from 0.7 to 2.2 m, and in each location, the radar is rotated to make AOA, α , equals to 0, 30, and 60 degrees separately.

The frame rate of the radar is set as 10 frames per second, the range resolution is set as 0.044 m, the maximum unambiguous range is set as 9.02 m, and the maximum radial velocity is set as 1 m per second. The software used to detect the object is mmWave Demo Visualizer 3.5, provided by Texas Instruments. It uses the Constant false alarm rate (CFAR) algorithm to detect the object. The radar uses this software to plot the relative RSSI for different objects with different distances. The received power and distances of the

objects can be used for modeling the received signal strength indicator (RSSI). In this software, people can set parameters such as the number of frames per second, the threshold for the algorithm to detect the object, etc., and read the relative power and the distance of the target.

Figure 4a shows the results received by mmWave Demo Visualizer that is accessible in [14]. The blue line represents the power of the signal, the green line represents the noise floor, and the orange points represent the detected objects. It is shown in Fig. 4a that when the IEEE 802.11ad communication is turned off, the radar can detect multiple objects with different distances. Figure 4b shows that when the IEEE 802.11ad communication is turned on, it reduces the SINR of strong targets and buries weak targets.

3.2 An Empirical Models for SIR

In the tests conducted in the laboratory, the detected object is IEEE 802.11ad TX, therefore, the RCS is fixed in the experiment. The model of received signal strength of radar is shown in Fig. 5a, where P_s is the power of received signal strength of radar. According to (8), we assume the model has an ideal path loss exponent, and the component, $10 \log_{10} P_r G_{TX} \sigma G_{RX} \lambda_r^2 / (4\pi)^3$, is gotten through linear fit. The model is

$$P_s(dB) = -40 \log_{10} r + 101.7 \tag{11}$$

where r is the distance between the radar and a target. In this model, the mean value of the shadow fading is -0.04 dB, and the standard deviation of the shadow fading is 3.78 dB.

In our laboratory tests, the radar is moved away from the RX and rotated to make AOA, α , equals $0, 30,$ and 60 degrees respectively. The P_I model in dB is shown in Fig. 5b. Based on (9), the interference path loss exponent will be 2, and based on Fig. 5b the overall interference path loss model is

$$P_I(dB) = -20 \log_{10}(r) + 22 \log_{10}(\cos(\alpha)) + 73.06 \tag{12}$$

where r is the distance between the radar and the TX, and α is AOA, whose range is restricted from 0 to 60 degrees because the azimuth field of view of the mmWave radar is 120 degrees. In this model, the mean value of the shadow fading is 0.004 dB, the standard deviation of the shadow fading is 1.07 dB. In (7), the coefficient of $\cos(\alpha)$ represents the relationship between AOA and the antenna gain of RX, which is modeled based on the datasheet of IWR6843AOPEVM radar [15].

The SINR is calculated from (10), based on the P_s model and P_I model. As the typical signal to noise ratio (SNR) value requirement for detecting the target is from 15 to 20 dB. We assume the SNR that is needed to detect the object is 20 dB and analyze the influence of the range the radar can detect when the IEEE 802.11ad communication is introduced. Figure 6 shows the SIR model. When the

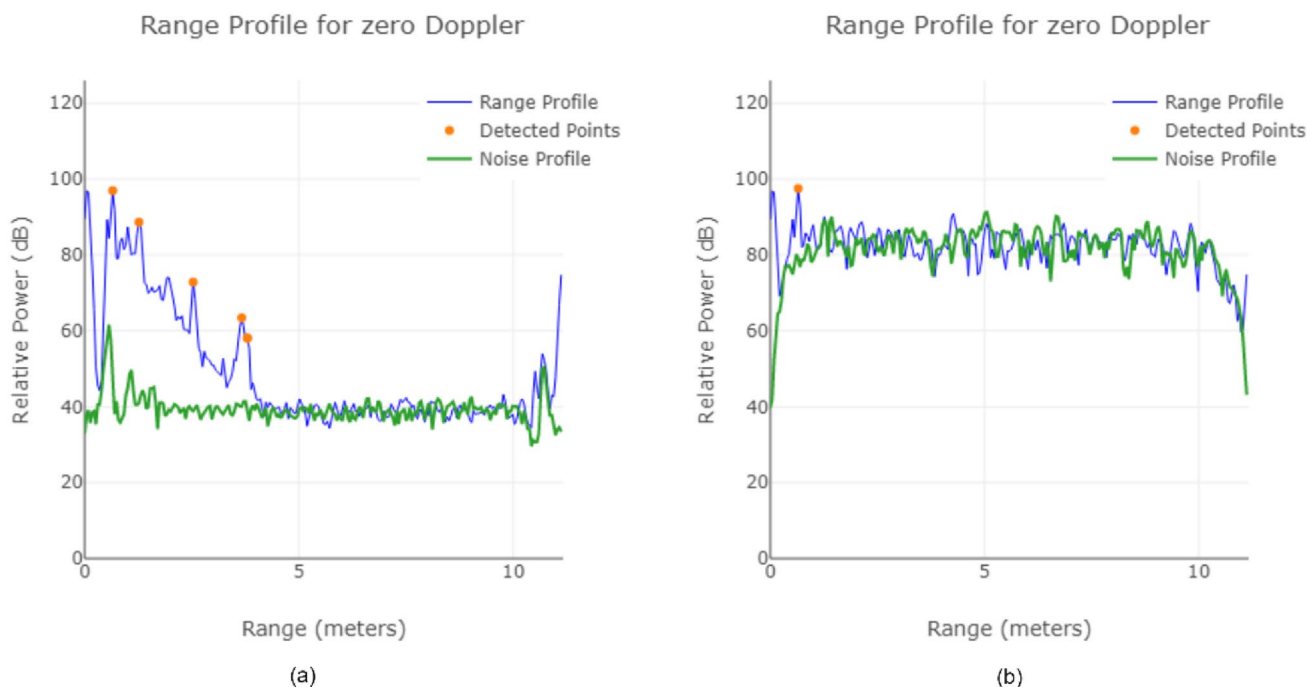


Fig. 4 Relative power of the detected objects a turn off the IEEE 802.11ad communication, b turn on the IEEE 802.11ad communication

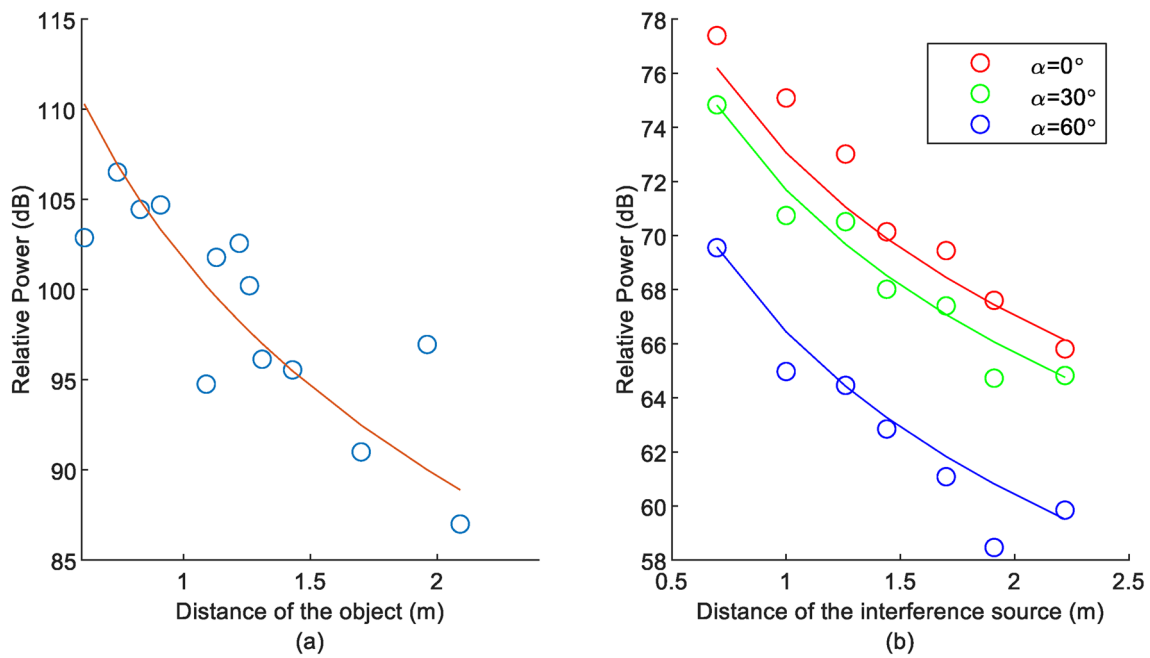


Fig. 5 a Power of signal model in the laboratory scenario b Power of interference model in the laboratory scenario

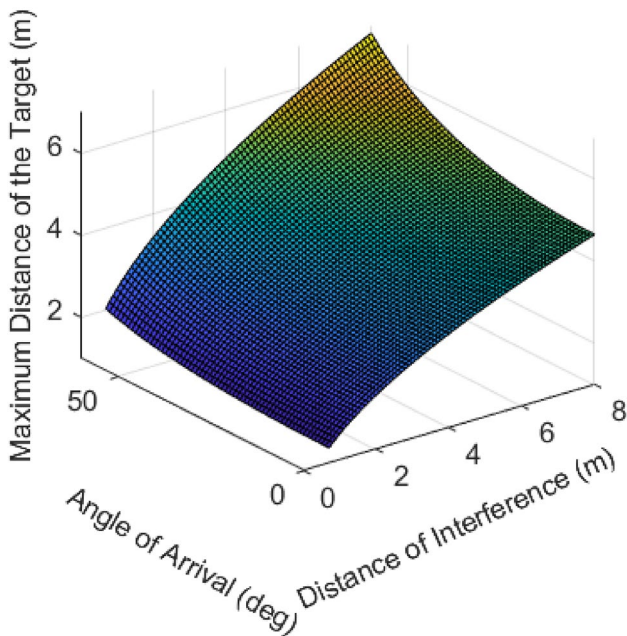


Fig. 6 The coverage of the mmWave radar under the IEEE 802.11ad communication when the SIR is 20 dB

interference source is close to the radar, the detection range decreases significantly.

3.3 CRLB for Precision of the Radar

To analyze the influence of the accuracy of the radar, we use Cramer–Rao lower bound (CRLB). In classical estimation theory, ranging and positioning are estimated based on single or multiple parameters, and CRLB is a mean for the calculation of the variance of those parameters [16]. In [17, 18], the CRLB of the FMCW radar is

$$CRLB = \text{var}(r) \geq \frac{3c^2}{(2\pi)^2 \times SNR \times NW^2} \tag{13}$$

where c is the speed of light, SNR is the signal to the noise ratio, N is the number of samples taken in the observation window, W is the bandwidth of the radar. In this scenario, we assume the distribution of the IEEE 802.11ad communication signal is the same as the thermal noise. The power of the thermal noise is neglected because it is far less than the power of interference. Therefore, when the interference is introduced, the CRLB is

$$CRLB = \text{var}(r) \geq \frac{3c^2}{(2\pi)^2 \times SIR \times NW^2} \tag{14}$$

The distance measurement error (DME) is

$$DME = \sqrt{CRLB} \tag{15}$$

Given that the SNR for object detection is 20 dB, the CRLB and the DME can be calculated using (14) and (15), respectively. As shown in (7), R_{res} of FMCW radar

is independent of SNR and therefore interference doesn't change the range resolution. Based on the set parameters, range resolution is in the order of 0.04 m, while the DME reduces with SNR, and it is in the order of 10^{-4} m. Thus, DME is much less than range resolution and the impact of interference on range estimation would not be detectable.

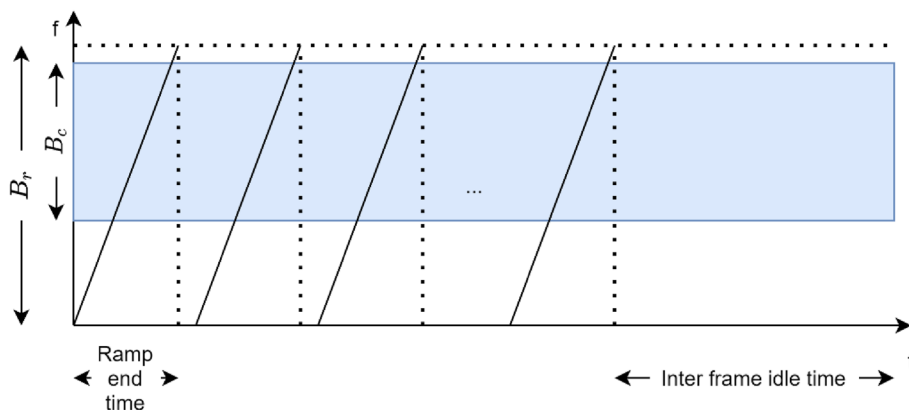
4 mmWave Radar Interference to IEEE 802.11ad

The interference applied by mmWave radar to IEEE 802.11ad causes packet losses. Indeed, when the radar is on and operates in the same band as the IEEE 802.11ad the transmitted packets will be corrupted, and the packets will be counted as lost packets. As a result, we can establish a timing diagram to calculate the theoretical PLR caused by interference from the mmWave radar. To validate these results, we need a testbed to measure the packet loss rate. In this section, we first present a theoretical foundation for calculation of the effects of mmWave radar interference on PLR of the IEEE 802.11ad, then we introduce a testbed for validation of the theoretical foundation.

4.1 A Theoretical Foundation for Interference of Radar into IEEE802.11ad

In this paper, the IEEE 802.11ad device works on the SC mode, the center frequency is 62.64 GHz, and the bandwidth is 2.16 GHz. The TI mmWave radar is working on the band from 60 to 64 GHz. The interference time ratio model is introduced to analyze the interference between FMCW radar and communication [8]. The interference time ratio model is shown in Fig. 7. B_c represents the bandwidth of the IEEE 802.11ad communication, B_r is the bandwidth of mmWave radar. For the radar, every frame has 48 chirps, ramp end time is the sweep time for one chirp. Between each chirp, it has an inter-chirp idle time, and between each frame, it has an inter-frame idle time.

Fig. 7 The sawtooth waveform of the millimeter-wave radar occupies B_r bandwidth and IEEE 802.11ad occupies B_c bandwidth. When their frequencies overlapped with each other, IEEE 802.11ad gets interference from the radar signal



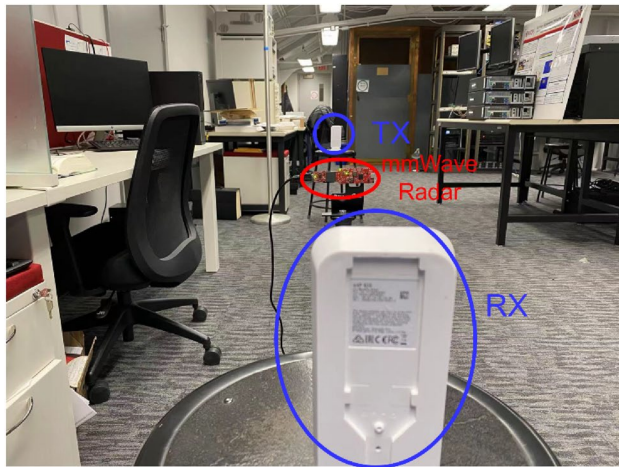
The interference time ratio is the time ratio in one frame that the frequency bands of mmWave radar and IEEE 802.11ad communication are overlapped. As the radar is set close to the RX of IEEE 802.11ad communication, the power of interference is very high compared to the RSSI of the communication signal. Assuming that their frequency bands overlap, the packets will get lost, and the packet loss rate (PLR) is approximately equal to the interference time ratio and can be written as

$$PLR \approx \frac{\frac{B_c N_c}{B_r}}{t_f} = \frac{\frac{B_c N_c}{B_r}}{\frac{1}{r_f}} \tag{16}$$

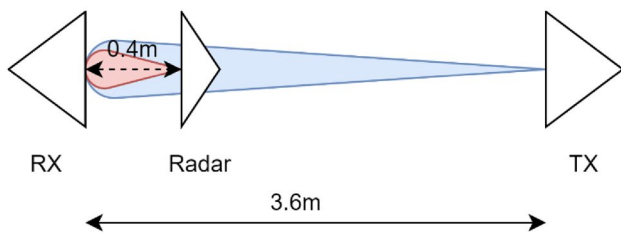
where B_c is the bandwidth of IEEE 802.11ad, B_r is the bandwidth of mmWave radar, N_c is the number of chirps in one frame, t_f is the duration of the frame, and r_f is the frame rate.

4.2 Empirical PLR for Validation of the Theoretical Foundation

In this scenario, as is shown in Fig. 8, the IEEE 802.11ad TX and RX are set 3.6 m apart in the laboratory. The distance between the radar and RX is 40 cm. To increase interference from radar to IEEE 802.11ad, the time ratio when the frequency bands of IEEE 802.11ad and mmWave radar are overlapped should be increased. As a result, the working time per second of the radar should be increased through changing the frame rate of the radar is changed from 10 frames per second to 30 frames per second. Besides, to make the radar has a longer working time in every chirp, the ramp end time for every chirp is set as high as 200 μ s, the inter-chirp idle time is as short as 8 μ s, and the default number of chirps in one frame is set as 48 according to the setting of the datasheet. For the IEEE 802.11ad communication, the payload of the packet is set as 6000 Bytes, and the packet loss rate is measured under the UDP protocol. The software Iperf3 was used to measure the packet loss rate. The measurement time is 30 s, and the average value of 10



(a)



(b)

Fig. 8 Scenario for the TI mmWave radar interference to the IEEE 802.11ad communication link. **a** The mmWave radar is set close to the IEEE802.11ad RX as the interference source. **b** The distance between the mmWave radar and the IEEE802.11ad RX is set as 0.4 m, and the distance between the IEEE802.11ad TX and RX is 3.6 m

measurements is the experimental result in this experiment. When the interference is not introduced, the analytical result of the packet loss rate is 0, the experimental result of the packet loss rate is 0.0579%. Table 1 shows the analytical and experimental packet loss rates when we introduced the interference based on different frame rates. Figure 9 shows the relation between the packet loss rate and the frame rate of the radar. The experimental results are distributed around the analytical results.

Table 1 Analytical and experimental packet loss rates of the IEEE 802.11ad communication based on different configurations of mmWave radar

Frames per second	Ramp end time (μ s)	Inter-chirp idle time (μ s)	Inter-frame idle time (ms)	Packet loss rate (Analytical)	Packet loss rate (Experiment)
10	200	8	90.02	5.18%	3.23%
15	200	8	56.68	7.78%	6.58%
20	200	8	40.02	10.37%	8.60%
25	200	8	30.02	12.96%	13.42%
30	200	8	23.35	15.55%	18%

5 Future Work

In the future work, we will set the testbed in different scenarios, such as corridors, open area, anechoic chamber, faraday cage, etc., to test the interference between mmWave radar and IEEE 802.11ad. The mitigation techniques which are used to improve the performance of mmWave radar and IEEE 802.11ad systems under interference should be analyzed in different scenarios to fully understand isolated and combined effect of various environmental parameters such as reflection and scattering.

6 Conclusion

In this paper, the interference between IEEE 802.11ad and mmWave radar is analyzed. To analyze IEEE 802.11ad interference to mmWave radar, we build the P_S and P_I models of the radar within the laboratory environment and use SINR and CRLB to explain the influence on the range and the accuracy on the radar performance. As the RCS of the object is fixed, when the interference from IEEE 802.11ad communication is introduced, the detection range of the radar decreases. Specifically, when the distance between the IEEE 802.11ad TX and the mmWave radar is 0.4 m with a 0-degree AOA, the detection range decreases from 9 to 1 m, and the accuracy for the detected objects will not change. To analyze the mmWave radar interference to IEEE 802.11ad communication, the interference time ratio model is introduced. When the frequency bands of IEEE 802.11ad and mmWave radar overlap, the IEEE 802.11ad communication will interfere. When the frame rate of the radar is increased from 10 frames per second to 30 frames per second, the theoretical ratio of time when the frequency bands of IEEE 802.11ad and radar increases. As a result, the theoretical packet loss rate increases from around 5–15%. The experimental results are close to the theoretical results. When the frame rate is 30 frames per second, the ramp end time is 200 μ s, the packet loss rate increases up to 15%.

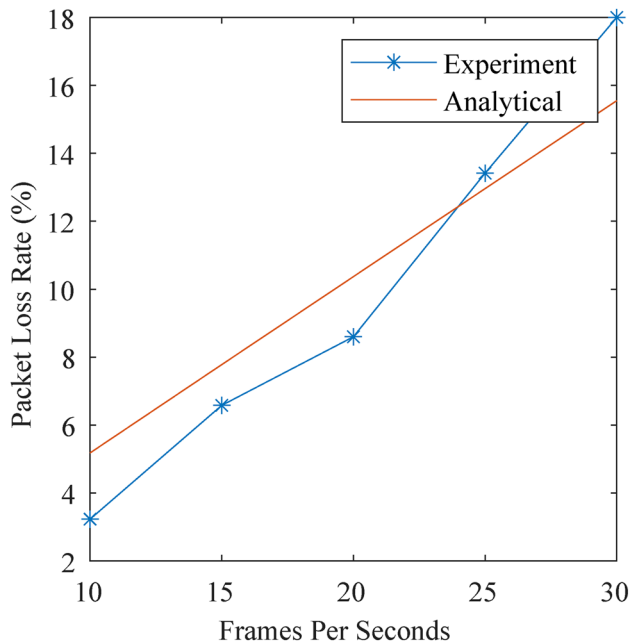


Fig. 9 Analytical and experimental results of the IEEE 802.11ad packet loss rate under the interference from mmWave radar at different frame rates

Funding This study was supported by the National Science Foundation, NSF SII-2037782, Kaveh Pahlavan

References

- BEST-NEST Invitational Online Workshop on New Paradigms in Intelligent Spectrum Management and Regulations, Future Directions, Technologies, Standards, and Applications. Dec 3–4, 2020, Webinar from WPI, Worcester, MA. Available: <https://bestnest.wpi.edu/index.php/synopsis-2/>
- T. Nitsche, C. Cordeiro, A. B. Flores, E. W. Knightly, E. Perahia and J. C. Widmer, IEEE 802.11ad: directional 60 GHz communication for multi-Gigabit-per-second Wi-Fi [Invited Paper], *IEEE Communications Magazine*, Vol. 52, No. 12, pp. 132–141, 2014. <https://doi.org/10.1109/MCOM.2014.6979964>.
- K. Pahlavan, J. Ying, Z. Li, E. Solovey, J. P. Loftus and Z. Dong, RF Cloud for cyberspace intelligence, *IEEE Access*, Vol. 8, pp. 89976–89987, 2020. <https://doi.org/10.1109/ACCESS.2020.2993548>.
- M. V. S. Chandrashekar, P. Choi, K. Maver, R. Sieber and K. Pahlavan, Evaluation of interference between IEEE 802.11b and Bluetooth in a typical office environment. 12th IEEE International Symposium on Personal, Indoor and Mobile Radio Communications. PIMRC 2001. Proceedings (Cat. No.01TH8598), 2001, pp. D-D. doi: <https://doi.org/10.1109/PIMRC.2001.965494>.
- J. H. Reed, et al., On the co-existence of TD-LTE and radar over 3.5 GHz band: an experimental study, *IEEE Wireless Communications Letters*, Vol. 5, No. 4, pp. 368–371, 2016. <https://doi.org/10.1109/LWC.2016.2560179>.
- A. Khawar and T. C. Clancy, A mathematical analysis of cellular interference on the performance of S-band military radar systems, *2014 Wireless Telecommunications Symposium*, 2014. <https://doi.org/10.1109/WTS.2014.6835028>.
- V. Deniau, C. Gransart, G. L. Romero, E. P. Simon and J. Farah, IEEE 802.11n communications in the presence of frequency-sweeping interference signals, *IEEE Transactions on Electromagnetic Compatibility*, Vol. 59, No. 5, pp. 1625–1633, 2017. <https://doi.org/10.1109/TEM.2017.2684428>.
- C. Aydogdu, M. F. Keskin, N. Garcia, H. Wymeersch and D. W. Bliss, RadChat: spectrum sharing for automotive radar interference mitigation, *IEEE Transactions on Intelligent Transportation Systems*, Vol. 22, No. 1, pp. 416–429, 2021. <https://doi.org/10.1109/TITS.2019.2959881>.
- J. Kim, S.-C. Kwon and G. Choi, Performance of video streaming in infrastructure-to-vehicle telematic platforms with 60-GHz radiation and IEEE 802.11ad baseband, *IEEE Transactions on Vehicular Technology*, Vol. 65, No. 12, pp. 10111–10115, 2016. <https://doi.org/10.1109/TVT.2016.2547943>.
- Z. Yang and A. Mani, *Interference mitigation for AWR/IWR devices*, Texas Instrument, Dallas, TX, USA, 2020.
- C. Iovescu and S. Rao, The fundamentals of millimeter wave sensors. Texas Instrument, Dallas, TX, USA, Tech. Rep., 2017, pp. 1–8. [Online]. Available: <https://www.ti.com/lit/pdf/spyy005>
- Antonucci, et al., Performance analysis of a 60-GHz radar for indoor positioning and tracking, *International Conference on Indoor Positioning and Indoor Navigation (IPIN)*, Vol. 2019, pp. 1–7, 2019. <https://doi.org/10.1109/IPIN.2019.8911764>.
- S. Rao and T. Instruments. Introduction to mmwave Sensing: FMCW Radars. [Online]. Available: https://training.ti.com/sites/default/files/docs/mmwaveSensing-FMCW-offlinevideo_wing_0.pdf (accessed: Apr. 19, 2022).
- T. Instruments, mmWave demo visualizer application. [Online]. Available: https://dev.ti.com/gallery/view/mmwave/mmWave_Demo_Visualizer/ver/3.5.0/ (accessed on 31 July 2021).
- IWR6843AOPEVM Datasheet. [Online] Available: <https://www.ti.com/lit/pdf/swrs237> (accessed on 31 August 2021).
- K. Pahlavan, *Indoor geolocation science and technology*, River Publishers, Copenhagen, Denmark, 2019.
- S. M. Kay, *Fundamentals of statistical signal processing: estimation theory*, Prentice-Hall, Upper Saddle River, NJ, USA, 1993.
- S. Scherr, S. Ayhan, M. Pauli and T. Zwick. Accuracy limits of a K-band FMCW radar with phase evaluation. 2012 9th European Radar Conference, 2012, pp. 246–249.

Publisher's Note Springer Nature remains neutral with regard to jurisdictional claims in published maps and institutional affiliations.



Shiyu Cheng received his bachelor's degree from Beihang University, China, in 2015. From 2020, he is pursuing the master's degree in the Center for Wireless Information Network Studies (CWINS) lab, Department of Electrical and Computer Engineering (ECE), Worcester Polytechnic Institute (WPI). His research interests include indoor localization, radio propagation channel modeling, and interference analysis.



Kaveh Pahlavan was a Westin Hadden Professor of electrical and computer engineering with the Worcester Polytechnic Institute (WPI), Worcester, MA, from 1993 to 1996. He is currently a Professor of electrical and computer engineering, a Professor of computer science, the Director of the Center for Wireless Information Network Studies, WPI, and the Chief Technical Advisor of Skyhook Wireless, Boston, MA. He has authored the books *Wireless Information Networks* (John Wiley and Sons, 1995),

Wireless Information Networks (John Wiley and Sons, Second Edition, 2005) (with Allen Levesque), *Principles of Wireless Networks—A Unified Approach* (Prentice Hall, 2002) (with P. Krishnamurthy), and *Networking Fundamentals: Wide, Local, and Personal Communications* (Wiley, 2009) (with P. Krishnamurthy). His current research interest includes opportunistic localization for body area networks and robotics applications. He received the Nokia Fellowship, in 1999, and the first Fulbright-Nokia Scholar with the University of Oulu, Finland, in 2000.



Haowen Wei is an Undergraduate Research Assistant at Worcester Polytechnic Institute (WPI) in CWINS Lab and HCI Lab majoring in ECE and CS class 2022. His research specialized in deep learning, machine learning, RF signals, and Human computer Interaction.



Zhuoran Su received the B.S. degree in communication engineering from Beijing Jiaotong University (BJTU), Beijing, China, in 2017, and the M.S. degree in electrical and computer engineering (ECE) from the Worcester Polytechnic Institute (WPI), Worcester, USA, in 2020, where he is currently continuing his research and pursuing the Ph.D. in ECE at WPI. His main fields of research interest are in indoor channel modeling, indoor localization, human motion detection and gesture

detection using RF signals, and deep learning using RF signals.



Seyed Reza Zekavat is a professor of Data Sciences and Physics of Worcester Polytechnic Institute. He is the Author of the textbook “*Electrical Engineering: Concepts and Applications*” published by Pearson, and the editor of the book “*Handbook of Position Location: Theory, Practice and Advances*,” published by Wiley/IEEE. He holds a patent on an active Wireless Remote Positioning System. Zekavat has also co-authored two books “*Multi-Carrier Technologies for Wireless Communications*,”

published by Kluwer, and “*High Dimensional Data Analysis*,” published by VDM Verlag; and 20 book chapters in the areas of adaptive antennas, localization, and spectrum sharing. Prof. Zekavat’s research interests are in wireless communications, positioning systems, software defined radio design, dynamic spectrum allocation methods, Radar theory, blind signal separation and MIMO and beam forming techniques, feature extraction, and neural networking. He is active on the technical program committees for several IEEE international conferences, serving as a committee chair or member. He has published more than 150 articles on these topics. He served on the editorial board of many Journals including *IET Communications*, *IET Wireless Sensor System*, and *Springer International Journal on Wireless Networks*. He has been on the Executive Committee of multiple IEEE conferences.



Ali Abedi received his PhD from University of Waterloo, Canada in 2004. He has been with the University of Maine, Orono since 2005, where he is currently Associate Vice President for Research and Professor of Electrical and Computer Engineering. He was visiting Associate Professor at the University of Maryland, College Park, MD, and Guest Researcher at NIST in 2012, and Faculty Fellow at NASA in 2016. Dr. Abedi is the founding Director of WiSe-Net Lab, where he directs research

programs including analytical performance evaluation of block codes, new methods for performance and convergence analysis of Turbo-codes, and applications of error correction codes in wireless sensor networks for structural monitoring, space explorations, and biomedical applications. His research on wireless sensing of lunar habitats was featured on the NSF Science360 website in 2012. Dr. Abedi has received a number of awards from the Natural Sciences and Engineering Research Council of Canada (NSERC), Japan Society for the Promotion of Science (JSPS), Canadian Space Agency (CSA), NASA, and IEEE. He is a senior member of IEEE and has served on several IEEE committees at local, regional, national, and international levels.

Terms and Conditions

Springer Nature journal content, brought to you courtesy of Springer Nature Customer Service Center GmbH (“Springer Nature”).

Springer Nature supports a reasonable amount of sharing of research papers by authors, subscribers and authorised users (“Users”), for small-scale personal, non-commercial use provided that all copyright, trade and service marks and other proprietary notices are maintained. By accessing, sharing, receiving or otherwise using the Springer Nature journal content you agree to these terms of use (“Terms”). For these purposes, Springer Nature considers academic use (by researchers and students) to be non-commercial.

These Terms are supplementary and will apply in addition to any applicable website terms and conditions, a relevant site licence or a personal subscription. These Terms will prevail over any conflict or ambiguity with regards to the relevant terms, a site licence or a personal subscription (to the extent of the conflict or ambiguity only). For Creative Commons-licensed articles, the terms of the Creative Commons license used will apply.

We collect and use personal data to provide access to the Springer Nature journal content. We may also use these personal data internally within ResearchGate and Springer Nature and as agreed share it, in an anonymised way, for purposes of tracking, analysis and reporting. We will not otherwise disclose your personal data outside the ResearchGate or the Springer Nature group of companies unless we have your permission as detailed in the Privacy Policy.

While Users may use the Springer Nature journal content for small scale, personal non-commercial use, it is important to note that Users may not:

1. use such content for the purpose of providing other users with access on a regular or large scale basis or as a means to circumvent access control;
2. use such content where to do so would be considered a criminal or statutory offence in any jurisdiction, or gives rise to civil liability, or is otherwise unlawful;
3. falsely or misleadingly imply or suggest endorsement, approval, sponsorship, or association unless explicitly agreed to by Springer Nature in writing;
4. use bots or other automated methods to access the content or redirect messages
5. override any security feature or exclusionary protocol; or
6. share the content in order to create substitute for Springer Nature products or services or a systematic database of Springer Nature journal content.

In line with the restriction against commercial use, Springer Nature does not permit the creation of a product or service that creates revenue, royalties, rent or income from our content or its inclusion as part of a paid for service or for other commercial gain. Springer Nature journal content cannot be used for inter-library loans and librarians may not upload Springer Nature journal content on a large scale into their, or any other, institutional repository.

These terms of use are reviewed regularly and may be amended at any time. Springer Nature is not obligated to publish any information or content on this website and may remove it or features or functionality at our sole discretion, at any time with or without notice. Springer Nature may revoke this licence to you at any time and remove access to any copies of the Springer Nature journal content which have been saved.

To the fullest extent permitted by law, Springer Nature makes no warranties, representations or guarantees to Users, either express or implied with respect to the Springer nature journal content and all parties disclaim and waive any implied warranties or warranties imposed by law, including merchantability or fitness for any particular purpose.

Please note that these rights do not automatically extend to content, data or other material published by Springer Nature that may be licensed from third parties.

If you would like to use or distribute our Springer Nature journal content to a wider audience or on a regular basis or in any other manner not expressly permitted by these Terms, please contact Springer Nature at

onlineservice@springernature.com